International Journal of Minerals*, *Metallurgy and Materials
Volume 22*, *Number 12*, *December 2015*, *Page 1260
DOI: 10.1007/s12613-015-1193-9

Slag formation path during dephosphorization process in a converter

Jiang Diao, Yong Qiao, Xuan Liu, Xie Zhang, Xin Qiu, and Bing Xie

College of Materials Science and Engineering, Chongqing University, Chongqing 400044, China

(Received: 8 October 2014; revised: 5 December 2014; accepted: 21 December 2014)

Abstract: The slag formation path is important for efficient dephosphorization in steelmaking processes. The phosphorus capacity and the melting properties of the slag are critical parameters for optimizing the slag formation path. Regarding these two factors, the phosphorus partition ratio was calculated using the regular solution model (RSM), whereas the liquidus diagrams of the slag systems were estimated using the FactSage thermodynamic package. A slag formation path that satisfies the different requirements of dephosphorization at different stages of dephosphorization in a converter was thus established through a combination of these two aspects. The composition of the initial slag was considered to be approximately 15wt%CaO–44wt%SiO_2–41wt%FeO. During the dephosphorization process, a slag formation path that follows a high-iron route would facilitate efficient dephosphorization. The composition of the final dephosphorization slag should be approximately 53wt%CaO–25.5wt%SiO_2–21.5wt%FeO. The composition of the final solid slag after dephosphorization is approximately 63.6wt%CaO–30.3wt%SiO_2–6.1wt%FeO.

Keywords: steelmaking; dephosphorization; slag composition; optimization

1. Introduction

Phosphorus is known as a harmful element in steels because it can induce cold brittleness [1−2]. Specially, for some low and ultralow phosphorous steels, dephosphorization in the steelmaking vessel prior to or after steelmaking is no longer sufficient. Hence in the 1990s, the duplex steelmaking process, which is characterized by the treatment of hot metal with two Linz-Donawitz (LD) converters (i.e., one for dephosphorization and another for decarburization), was developed in Japan [3−7]. Two noteworthy features of the duplex steelmaking process are the faster formation of slag because the shorter tap-to-tap time and the requirement of a high phosphorus capacity of the slag. Hence, the development of methods for accelerated slag formation in LD converters is challenging.

Wu *et al.* [8] studied the slag formation path of a combined blowing converter for medium- and low-phosphorus hot metal. Basu *et al.* [9] presented the slag formation path of a commercial basic oxygen furnace (BOF). The effect of ladle slag recovery and utilization in BOF on slag path was also discussed by Dahlin [10]. The slag formation path for hot metal with different Si contents was formulated by Swinnerton [11]. However, to the best of our knowledge, investigations of the slag formation path for the duplex steelmaking process and of the corresponding slag formation mechanism are scarce. To ensure highly efficient dephosphorization, rapidly increasing the phosphorus capability of slag while slowly increasing the melting temperature of slag during the dephosphorization process would be beneficial. Therefore, in the present study, we aimed to develop a suitable slag formation path for the dephosphorization process in a converter.

2. Methodology

The slag formation path in the BOF is briefly described. In general, two thermodynamic aspects of dephosphorization in a converter are relevant. One such aspect is the melting property of the dephosphorization slag. The CaO–SiO_2–FeO system is the most widely used dephosphorization slag. The liquidus diagram of this system was calculated using the FactSage thermodynamic package with the Equilib module. The calculated temperature range was from 1573 to

---

Corresponding author: Jiang Diao E-mail: diaojiang@163.com

1773 K in steps of 100 K. The effects of MgO and MnO on the melting temperature of the dephosphorization slags were also calculated using the FactSage program. In the calculations, the total mass ratio for CaO, SiO_2, and FeO was 1, whereas the mass ratios of other components were calculated using the following equation:

$$c(\mathrm{M}_x\mathrm{O}_y)=\frac{w(\mathrm{M}_x\mathrm{O}_y)}{w(\mathrm{CaO})+w(\mathrm{SiO}_2)+w(\mathrm{FeO})} \tag{1}$$

where M_xO_y denotes MnO, MgO, or P_2O_5 and $w(M_xO_y)$ indicates the mass fraction of M_xO_y in the slag; $c(M_xO_y)$ is the relative mass percentage of M_xO_y in the slag.

Another important aspect is the dephosphorization ability. As the slag composition changes during oxidation, so does the phosphorus capacity of the slags. The effect of this evolution of phosphorus capacity on dephosphorization is a topic of great interest. Hence, the construction of a thermodynamic model to evaluate the phosphorus capacity of the dephosphorization slag and to further contribute to determining the reasonable range of slag composition for dephosphorization is worthwhile. The regular solution model (RSM) has been widely used because of its numerous advantages. In particular, it is well suited for dealing with the equilibrium partition ratio of the oxygen, phosphorus, and sulfur between slag and liquid steel. Hence, the equilibrium phosphorus partition ratio (L_P) with respect to chemical composition and temperature was calculated via the RSM:

$$2[\mathrm{P}]+5(\mathrm{FeO})=(\mathrm{P}_2\mathrm{O}_5)+5[\mathrm{Fe}] \tag{2}$$

$$K^0=\frac{\gamma_{\mathrm{P}^{5+}}^2[x(\mathrm{P}^{5+})]^2}{(w[\mathrm{P}])^2\cdot\gamma_{\mathrm{Fe}^{2+}}^5[x(\mathrm{Fe}^{2+})]^5} \tag{3}$$

$$L_\mathrm{P}=\frac{w(\mathrm{P})}{w[\mathrm{P}]}=\frac{w(\mathrm{P})\cdot(K^0)^{0.5}\cdot[x(\mathrm{Fe}^{2+})]^{2.5}\cdot\gamma_{\mathrm{Fe}^{2+}}^{2.5}}{x(\mathrm{P}^{5+})\cdot\gamma_{\mathrm{P}^{5+}}} \tag{4}$$

where the square brackets and parentheses denote the metal phase and slag phase, respectively; $w(P)$ and $w[P]$ denote the mass percent of P in slag phase and metal phase; $x(P^{5+})$ and $x(Fe^{2+})$ denote the molar fraction of P^{5+} and Fe^{2+}, respectively; γ is the activity coefficient; K^0 is the equilibrium constant of the reaction (0.0234) [12] and is independent of the temperature; and L_P is the equilibrium phosphorus partition ratio.

3. Results and discussion

3.1. Melting properties of the CaO–SiO_2–FeO–(MgO, MnO, P_2O_5) slag systems

The calculated liquidus diagram of the CaO–SiO_2–FeO slag system shown in Fig. 1 is in good agreement with the reported liquidus diagram of the CaO–SiO_2–FeO slag system [13], which demonstrates that the calculation method is reliable. The liquidus diagrams of different slag systems were obtained under the assumption that 5wt% MgO, 5wt% MnO, and 8wt% P_2O_5 (considering high-P hot metal) were added to the CaO–SiO_2–FeO slag system. The results are shown in Figs. 2(a)–2(d). A comparison of Fig. 1 to Fig. 2(a) reveals that the liquidus region increased with increasing MgO content. In addition, a comparison of Fig. 1 with Fig. 2(b) indicates that the liquidus region increased when MnO was added to the slag. In practical dephosphorization processes, a certain content of these oxides in the slag are beneficial for dephosphorization. A comparison of Figs. 2(c) and 2(d) also indicates that the liquidus region increased when P_2O_5 was added to slag, consistent with the results reported by Zhao *et al.* [14]. Hence, the melting temperature of the dephosphorization slag was decreased by the addition of such additives; this decrease in melting temperature promotes the melting of the slag and the mass transfer of phosphorus between the slag and metal.

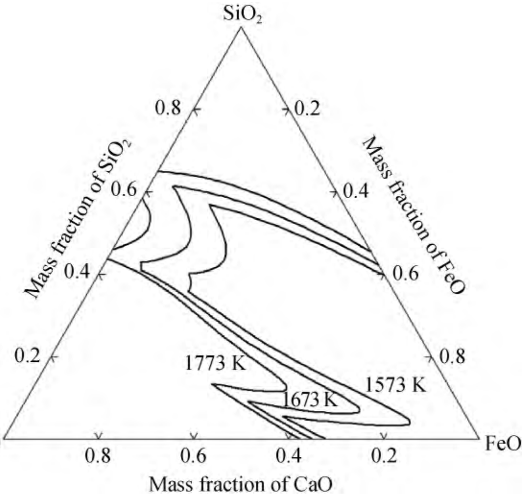

Fig. 1. Liquidus diagram of the CaO–SiO_2–FeO slag system.

Fig. 3 shows the relationship between the MgO content and the melting temperature of the CaO–SiO_2–FeO–MgO system. When w(MgO) was increased from 0 to 5wt%, the melting temperature of the slag decreased; however, when w(MgO) exceeded 5wt%, the melting temperature increased. If only the melting property of the slag is considered, control of the MgO content in the range of 3wt%–5wt% of the slag composition is preferred.

Given that the utilization of decarburization slag (with a certain amount of MnO, 14wt%–30wt% [15]) in dephosphorization converters favors the formation of slag and benefits dephosphorization, we also calculated the effect of MnO content in the slag on the melting temperature of the CaO–SiO_2–FeO–MgO–MnO–P_2O_5 slag system using the

FactSage program. As shown in Fig. 4, with an increase in w(MnO) in the range of 3wt%–12wt%, the melting temperature decreased slightly, which means that MnO could promote the melting of dephosphorization slag.

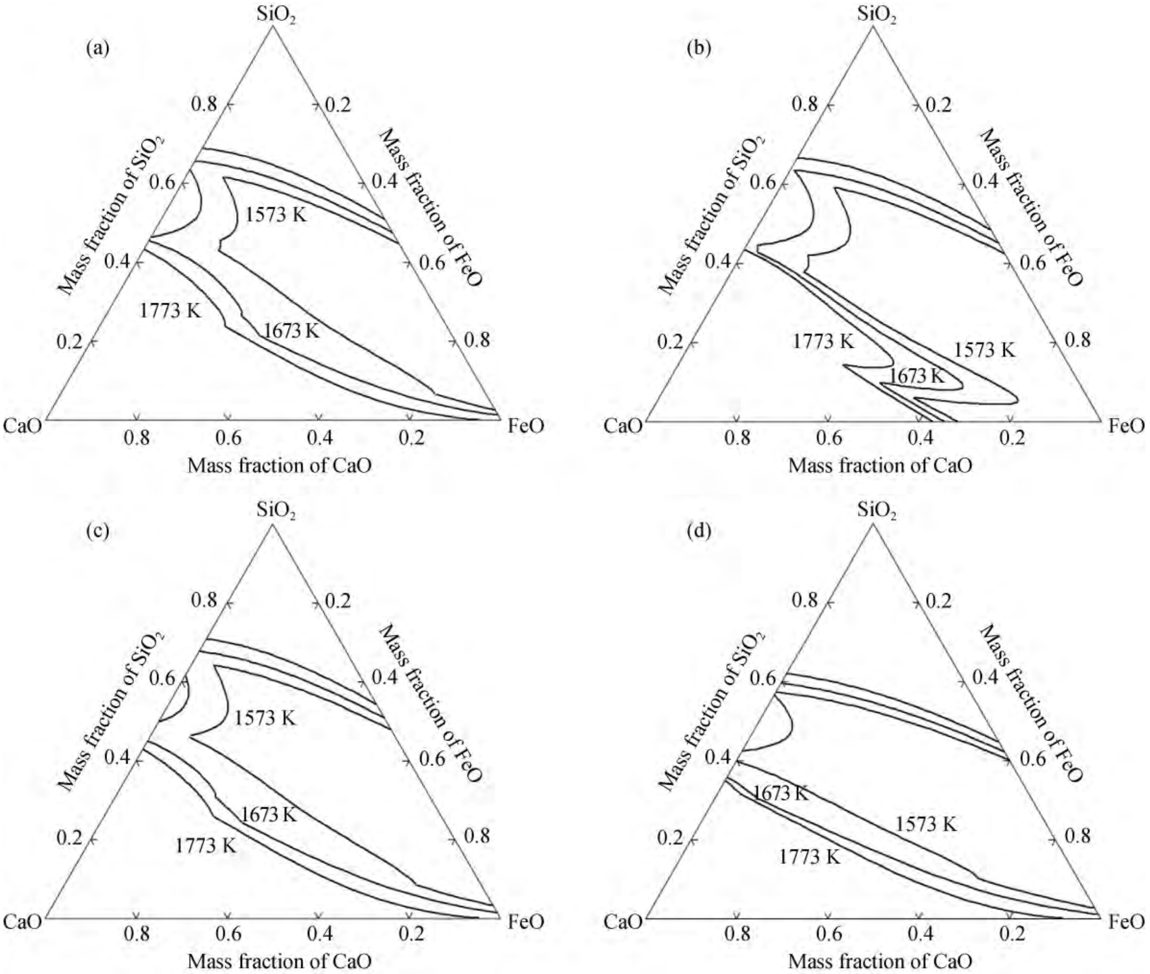

Fig. 2. Liquidus diagrams of CaO–SiO$_2$–FeO–(MgO, MnO, P$_2$O$_5$) slag systems: (a) CaO–SiO$_2$–FeO–MgO, $w(\mathrm{MgO})/(w(\mathrm{CaO})+w(\mathrm{SiO_2})+w(\mathrm{FeO}))=0.0526$; (b) CaO–SiO$_2$–FeO–MnO, $w(\mathrm{MnO})/(w(\mathrm{CaO})+w(\mathrm{SiO_2})+w(\mathrm{FeO}))=0.0526$; (c) CaO–SiO$_2$–FeO–MgO–MnO, $w(\mathrm{MgO})/(w(\mathrm{CaO})+w(\mathrm{SiO_2})+w(\mathrm{FeO}))=0.056$, $w(\mathrm{MnO})/(w(\mathrm{CaO})+w(\mathrm{SiO_2})+w(\mathrm{FeO}))=0.056$; (d) CaO–SiO$_2$–FeO–MgO–MnO–P$_2O_5$, $w(\mathrm{MgO})/(w(\mathrm{CaO})+w(\mathrm{SiO_2})+w(\mathrm{FeO}))=0.061$, $w(\mathrm{MnO})/(w(\mathrm{CaO})+w(\mathrm{SiO_2})+w(\mathrm{FeO}))=0.061$, $w(\mathrm{P_2O_5})/(w(\mathrm{CaO})+w(\mathrm{SiO_2})+w(\mathrm{FeO}))=0.0976$.

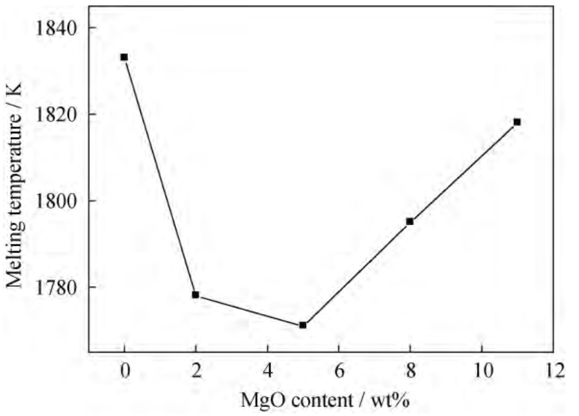

Fig. 3. Melting temperatures of the CaO–SiO$_2$–FeO–MgO system (w(CaO)/w(SiO$_2$) = 2.1, FeO 20wt%).

3.2. Dephosphorization ability of the CaO–SiO$_2$–FeO–MgO–MnO–P$_2$O$_5$ slag system

The phosphorus partition ratio between the slag and hot metal of the CaO–SiO$_2$–FeO–4wt%MgO–7wt%MnO–7wt%P$_2$O$_5$ slag system at 1623 K is presented in Fig. 5. In the dephosphorization process, high dephosphorization capability is favored. A high-efficiency slag formation path for dephosphorization should guarantee a continuous increase in L_P during the dephosphorization process. The combination of Fig. 2(d) and Fig. 5 revealed that a path exists where the L_P increases dramatically with the variation of slag composition during dephosphorization while the melting temperature of slag simultaneously increases slowly, which is beneficial for the quick melting of the slag and promotes the formation of the dephosphorization slag as well. On the basis of these insights, a slag formation path for the dephosphorization process can be constructed.

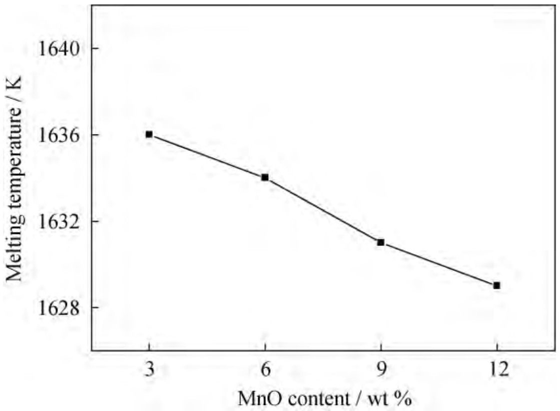

Fig. 4. Melting temperatures of the CaO–SiO$_2$–FeO–MgO–MnO–P$_2$O$_5$ system (w(CaO)/w(SiO$_2$) = 2.1, FeO 20wt%, MgO 4wt%, P$_2$O$_5$ 5wt%)

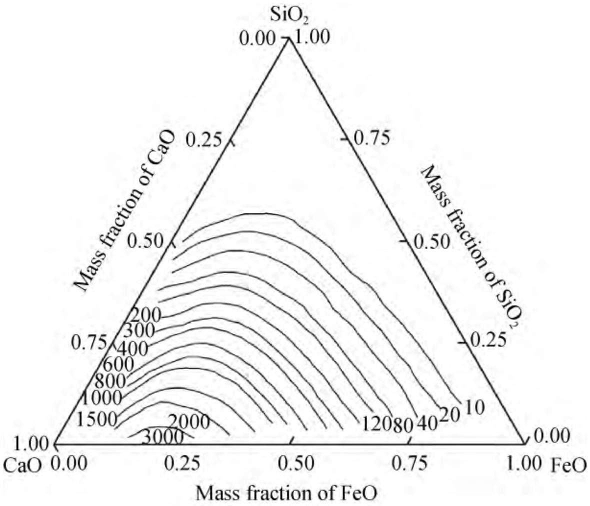

Fig. 5. Contour map on L_P of the CaO–SiO$_2$–FeO–MgO–MnO–P$_2$O$_5$ slag system (MgO 4wt%, MnO 7wt%, P$_2$O$_5$ 7wt%)

3.3. Slag composition control in a dephosphorization converter

The evolution of slag composition at four different steel plants is presented in Fig. 6. Path I shows the slag evolution reported by Cicutti *et al.* [16]. At the beginning of the process, the slag has a low basicity and a relatively high FeO content, allowing lime to be dissolved into the slag. Near the middle of the process, an obvious decrease in the FeO content is observed, which almost coincides with the period of maximum decarburization of the bath. Toward the end of the process, most of the carbon has been removed from the bath; as a consequence, the oxygen blowing forms FeO that is incorporated into the slag, which promotes an increase in the FeO content in the final slag. Three other slag formation paths in Fig. 6 are similar to Path I. These paths are the most commonly used slag formation path in conventional converters. Although some differences exist in slag composition at the beginning and end of the paths because of the different operating conditions, the evolution rule of slag composition is consistent.

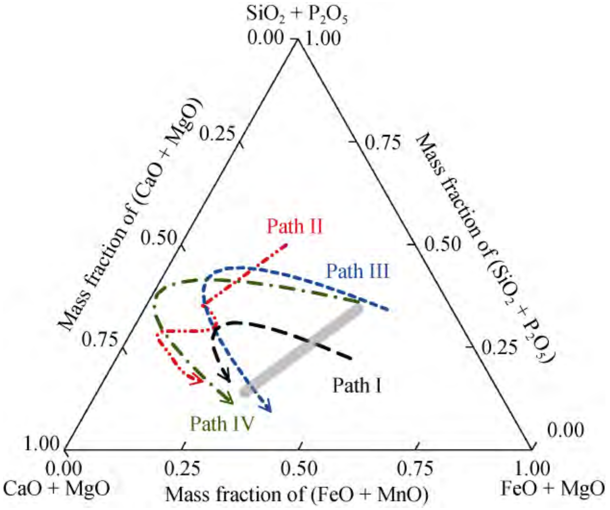

Fig. 6. Changes in slag composition for various converter practices (I, Cicutti *et al.* [16]; II, Basu *et al.* [9]; III, Swinnerton [11]; IV, Kreijger *et al.* [17]).

Theoretically, the gray line in Fig. 6 is the shortest slag formation path; however, it requires a rapid increase in temperature during the smelting process, which would induce a vigorous chemical reaction and adversely affect dephosphorization. The conventional slag formation path, which is represented by paths I–IV, is not suitable for dephosphorization in a converter because the blowing time in a dephosphorization converter is shorter than that in a conventional steelmaking converter. Moreover, the temperature at the end of dephosphorization process is far lower (by approximately 300°C) than that at the end of steelmaking. Therefore, the slow melting speed of lime would lead to a slow increase in the slag basicity; thus, the slag is not easily melted, which does not favor dephosphorization and can even easily cause weak fluidity of the slag during the medium blowing stage.

Fig. 7 shows a theoretical slag formation path *ABCD* in a dephosphorization converter. This path is based on two factors: melting properties and dephosphorization ability. At the beginning of dephosphorization, the slag should have a low melting temperature, which is beneficial for melting the slag and preparing for dephosphorization. In the present study, a typical chemical composition of point *A* is estimated as 15wt%CaO–41wt%FeO–44wt%SiO_2. We determined the melting temperature of such a slag (15wt%CaO–41wt%FeO–44wt%SiO_2 with 4wt% MgO, 7wt% MnO, and 7wt% P_2O_5) using the hemisphere point method. The melting point is approximately 1259°C. Therefore, the region around point *A* has a very low melting temperature and is thus well suited to be the initial slag because it favors the quick formation of the dephosphorization slag. In addition, the content of FeO around point *A* is approximately 40wt%, which is beneficial for melting lime and accelerating the formation of the dephosphorization slag.

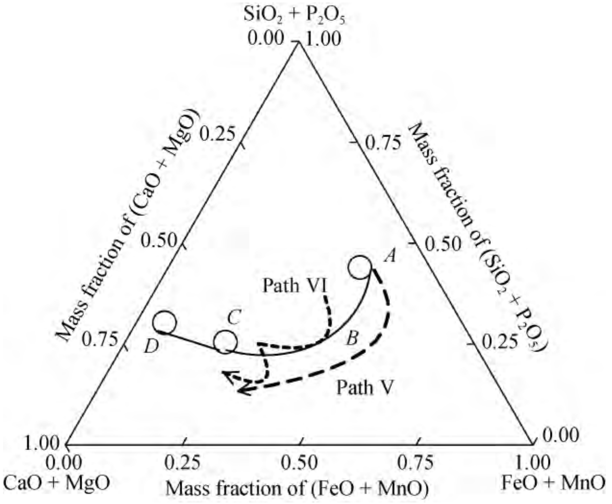

Fig. 7. Theoretical slag formation path in a dephosphorization converter (V, Wang *et al.* [18]; VI, Li [19]).

At the medium dephosphorization stage, a slag with a low melting point and a high phosphorus capacity would be beneficial because it would ensure a high dephosphorization rate. Therefore, improving the FeO content in the slag to further benefit the melting of lime to form high-basicity slag is important. Hence, the slag formation path should proceed through region *B* such that the FeO content increases and the basicity correspondingly increases slowly. Path V, which was reported by Wang *et al.* [18], is a desirable slag formation path for double slag operation in a BOF. Given the similarity between the double-slag process and the duplex steelmaking process, the first halves of path V and path *ABC* are approximately the same. Path VI, which was reported by Li [19], is a slag formation path for high-phosphorus hot-metal refining in a 50-t BOF. The first half of the path is the dephosphorization period, which is also in agreement with path *ABC*. A previous industrial test using 200-kg experimental furnace and 350-t BOFs also showed the same evolution rule of FeO content in slag [20].

At the end of dephosphorization, an efficient dephosphorization slag with high basicity is required to keep the phosphorus in the slag. Figs. 6 and 7 show that both the slag basicity and the FeO content in the dephosphorization process are lower than those in the conventional slag formation path [21] because of the favorable thermodynamic conditions of low temperature in the dephosphorization converter. Such conditions mean that a high alkalinity and high FeO content are no longer necessary. Actually, the slag basicity in a dephosphorization converter cannot reach 3–5 because of the short blowing period. The chemical composition of slag at point *C* is approximately 53wt%CaO–25.5wt%SiO_2–21.5wt%FeO, and the basicity is approximately 2.1. The melting temperature of such a slag is greater than 1370°C, as determined using hemisphere point method. Therefore, the slag composition region around point *C* is available to bind P_2O_5 in the slag. Before taping semi-steel, two aspects should be taken into consideration: the Fe content in the slag should be reduced to decrease the loss of iron; however, the formation of a solid slag is preferred to prevent the phosphorus transferring from the slag back to the semi-steel. For this purpose, the slag at point *D* is an excellent choice. The chemical composition of the slag at point *D* is approximately 63.6wt%CaO–30.3wt%SiO_2–6.1wt%FeO. The line *ABCD* is the optimum slag formation path during the dephosphorization process for the duplex steelmaking process. In the practical smelting process, the variation of the chemical composition of the slag from *C* to *D* can be achieved by controlling the oxygen blowing process.

Fig. 8 shows the relationship between L_P adapted from our previous study [22] and slag composition. The phosphorus partition ratio between the slag and metal was observed to vary between 10 and 51 and the basicity of the slag was observed to range from 1.5 to 2.1 at 1370°C. In

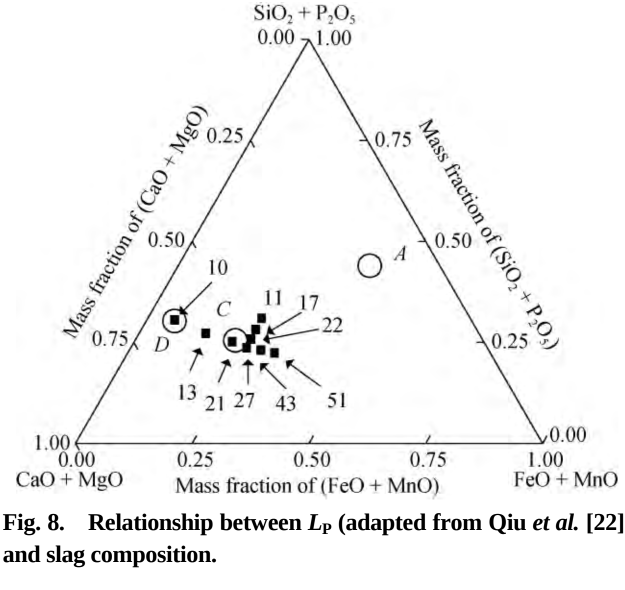

Fig. 8. Relationship between L_P (adapted from Qiu *et al.* [22]) and slag composition.

addition, L_P was observed to increase with increasing basicity and increasing FeO content in the slag. The region around point *C* on the slag formation path is a desirable slag composition for dephosphorization in a converter.

4. Conclusion

To strengthen the dephosphorization process in a converter, a high-efficiency dephosphorization slag formation path should be constructed. The melting property of the slag was calculated using the FactSage program, and its dephosphorization ability was calculated using the RSM. The slag formation path for dephosphorization was thus obtained by coupling the liquidus temperature and dephosphorization capability of the slag. The composition of the initial slag was considered to be approximately 15wt%CaO–44%wtSiO_2–41wt%FeO. During the dephosphorization, a slag formation path that follows a high-iron route would facilitate efficient dephosphorization. The composition of the final dephosphorization slag should be approximately 53wt%CaO–25.5wt%SiO_2–21.5wt%FeO. The composition of the final solid slag for keeping phosphorus is approximately 63.6wt%CaO–30.3wt%SiO_2–6.1wt%FeO.

Acknowledgement

This work was partially supported by the Fundamental Research Funds for the Central Universities (No. CDJZR 14130001).

References

[1] P.C. Li and J.L. Zhang, A prediction model of phosphorus distribution between $CaO–SiO_2–MgO–FeO–Fe_2O_3–P_2O_5$ slags and liquid iron, *ISIJ Int.*, 54(2014), No. 4, p. 756.

[2] S.L. Xie, W.L. Wang, Y.Z. Liu, and H. Matsuura, Effect of Na_2O and B_2O_3 on the distribution of P_2O_5 between solid solution and liquid phases slag, *ISIJ Int.*, 54(2014), No. 4, p. 766.

[3] B.J. Monaghan, R.J. Romfret, and K.S. Coley, The kinetics of dephosphorization of carbon-saturated iron using an oxidizing slag, *Metall. Mater. Trans. B*, 29(1998), No. 1, p. 111.

[4] Y. Ogasawara, Y. Miki, Y. Uchida, and N. Kikuchi, Development of high efficiency dephosphorization system in decarburization converter utilizing Fe_tO dynamic control, *ISIJ Int.*, 53(2013), No. 10, p. 1786.

[5] S.Y. Kitamura, K. Yonezawa,Y. Ogawa, and N. Sasaki, Improvement of reaction efficiency in hot metal dephosphorisation, *Ironmaking Steelmaking*, 29(2002), No. 2, p. 121.

[6] K. Naito and M. Wakoh, Recent change in refining process in Nippon Steel Corporation and metallurgical phenomena in the new process, *Scand. J. Metall.*, 34(2005), No. 6, p. 326.

[7] T. Ohnishi, H. Takagi, T. Ogura, K. Hajika, T. Yabata, and Y. Yoshida, A pretreatment technique for hot metal using a newly-developed refining furnace, *Kobe Res. Dev.*, 36(1986), No. 1, p. 9.

[8] W. Wu, Z.S. Zou, Z.H. Guo, D.R. Wu, and G.G. Zhao, Optimum slag forming route for BOF with top and bottom blowing oxygen, *J. Iron Steel Res.*, 16(2004), No. 1, p. 21.

[9] S. Basu, A.K. Lahiri, S. Seetharaman, and J. Halder, Change in phosphorus partition during blowing in a commercial BOF, *ISIJ Int.*, 47(2007), No. 5, p. 766.

[10] A. Dahlin, *Influence of Ladle-slag Additions on BOF-process Parameters* [Dissertation], Royal Institute of Technology, Stockholm, 2011, p. 23.

[11] M. Swinnerton, *The Influence of Slag Evolution on BOF Dephosphorisation* [Dissertation], University of Wollongong, Wollongong, 2005, p. 22.

[12] X.H. Huang, *Ferrous Metallurgy Theory*, 3rd Ed., Metallurgical Industry Press, Beijing, 2002, p. 180.

[13] V.D. Eisenhüttenleute, *Slag Atlas*, 2nd Ed., Verlag Stahleisen GmbH, Düsseldorf, 1995, p. 126.

[14] J.X. Zhao, X.M. Li, J.L. Guo, and M. Huang, Study on effect of P_2O_5 in converter slag on hot metal dephosphorization, *China Metall.*, 18(2008), No. 10, p. 8.

[15] Y.C. Wen, Y.H. Dong, T. Wang, and D.X. Du, Study of manganese ore direct alloying for increasing [Mn] content in steel in steelmaking process, *Iron Steel Vanadium Titanium*, 19(1998), No. 3, p. 7.

[16] C. Cicutti, M. Valdez, T. Pérez, R. Donayo, and J. Petroni, Analysis of slag foaming during the operation of an industrial converter, *Lat. Am. Appl. Res.*, 32(2002), No. 3, p. 237.

[17] P.J. Kreijger and R. Boom, Slag formation in large scale BOF steelmaking, *Can. Metall. Q.*, 21(1982), No. 4, p. 339.

[18] X.B. Wang, M.X. Feng, Z.S. Zou, G.G. Zhao, and Z.X. Liu, Slag forming route and dephosphorization of BOF dephosphorizing pretreatment and direct Steelmaking, *Iron Steel*, 44(2009), No. 1, p. 23.

[19] W.C. Li, *Metallurgical Thermodynamics*, Metallurgical Industry Press, Beijing, 1995, p. 128.

[20] A. Matsui, S. Nabeshima, H. Matsuno, N. Kikuchi, and Y. Kishimoto, Kinetics behavior of iron oxide formation under the condition of oxygen top blowing for dephosphorization of hot metal in the basic oxygen furnace, *Tetsu-to-Hagane*, 95(2009), No. 3, p. 207.

[21] L.M. Sun, Duplex melting process of converter and its features, *Shanghai Met.*, 27(2005), No. 2, p. 44.

[22] X. Qiu, B. Xie, L. Jiang, X. Zhang, J. Diao, and H.Y. Li, Experimental study of phosphorus distribution between slag and metal during duplex dephosphorus converter processing, [in] *Proceedings of the 4th International Symposium on High-Temperature Metallurgical Processing*, San Antonio, 2013, p. 199.